How do the available density functionals perform on the calculation of eigenvalues of frontier to deeper orbitals? A metric space evaluation of experimental and quantum chemical findings

Demetrios Xenides, Panaghiotis Karamanis

How Do The Available Density Functionals Perform on The Calculation of Eigenvalues of Frontier to Deeper Orbitals? A Metric Space Evaluation of Experimental and Quantum Chemical Findings

Demetrios Xenides*,† and Panaghiotis Karamanis‡

†*Laboratory of Predictive Analytics and Complex Systems, Department of Economics, School of Management and Economics, University of Peloponnese, Tripolis Campus, 22100, Greece*

‡*E2S UPPA, CNRS, IPREM, Université de Pau et des Pays de l Adour, 64053 Pau, France*

E-mail: xenides@uop.gr

Abstract

The present endeavor has been inspired by the vital role of orbital energies, and not only the ones relating to electron affinities (EAs) or ionization potentials (IPs), in elucidating the electronic nature of chemical species and molecules via advanced spectroscopic studies. These often aided by Density Functional Theory (DFT) calculations. Thus, we offer a rigorous classification of a plethora of 45 functionals that have been implemented in calculations of 26 diverse reference chemical moieties. The DFT methods that incorporate a large amount of HF exchange seem to recover a substantial part of HFs deficiency. The leading DFs are the long range corrected LC-ωHPBE or the

ones containing empirical dispersion only: ωB97, ωB97XD. Following the meta-GGA with a sufficient amount of HF exchange such as M05-2X, M06-2X, M08-HX, and the long range corrected M11, and the BMK as well.

Introduction

Currently, most of the published results in computational chemistry are being produced after performing Density Functional Theory (DFT) quantum chemical calculations. It is also a common place that DFT computational studies are routinely carried out not only by theoreticians but also by experimentalists. The latter group apply user friendly computational packages to support and elucidate their own laboratory findings. One of the numerous fields in which electronic structure calculations have become very popular among chemists is the calculation of eigenvalues of orbitals that, along with other, are holding a key role in molecular electronic structure and reactivity. Furthermore, they can be easily combined with powerful experimental techniques, as for example the widely applied ultra-violet - visible Photoelectron Spectroscopy (UV-VIS-PES) that is used for the elucidation of the electronic structure of molecules and materials. This is very well explained in recent studies by Morita and Eko[1] and Borges et al.,[2] and in the eloquent review by Ozaki et al.[3]

In the present study we worked towards a critical evaluation of the predictive capability of Density Functionals (DFs) in the calculation of that much of eigenvalues of Kohn-Sham (KS) orbitals as they are observed in PES studies. This is reasoned by the fact that such eigenvalues, which define the nature of a given chemical moiety, cannot be directly determined by any other higl level ab-initio approach. In particular, Moller-Plesser perturbation theory or coupled cluster approaches that comprise the treatment of dynamic electron correlation effects via standard perturbative techniques.

At this point it is fair to mention that electron affinities (EAs) and ionization potentials (IPs) via the corresponding HOMO and LUMO energies have extensively studied. In 2003 Zhan et al[4] implemented the B3LYP[5] functional in the calculation of HOMO and LUMO

orbitals in order to examine the role of the size of a basis set on the calculation of EAs and IPs. Later, Vydrov and Scuseria[6] performed calculations on IPs and EAs, targeting in comparison of the LC-ωPBE[7] functional to other commonly used functionals. Similar IPs and EAs calculations performed by Sun et al[8] on adenine-thymine nucleobase pairs showing that LC-DFT can reasonably describe the requested energies. Knight et al[9] introduced the GW methods,[10,11] (that is the self energy is calculated as a product of the Green function and the screened Coulomb interaction W) in similar orbital energies studies of molecules suitable for applications in organic electronics. Kang et al[12] have also calculated IPs and EAs to demonstrate the predictive capability of the combination of DFT and GW methods. We also mention a recent study in predicting band gaps via the DFT+U approach by Dabo et al.[13]

With the present study we moved this evaluation some steps further. Thus, except from the energy of the frontier orbitals, namely HOMO and LUMO, we have considered a larger set of eigenvalues of orbitals relying on available UV-Vis- photoelectron spectroscopic reference data of organic molecules bearing different bonding features.

To prepare the ground for such a study we first formed a set of reference compounds ranging from aliphatic hydrocarbons, alcohols and thioalcohols to ethers, amines, and chloro- or fluoro- substituted molecules, for which experimental data have been reported and analysed by means of UV-Vis-PES. Then, we carefully chose the "tools" for this evaluation, thus we relied on a purposely adapted metric space approach applied on results obtained by a representative group of functionals; from the oldest to more recently developed ones. Specifically, the present manuscript is organized as follows: In a first step, we briefly introduce the procedure we followed as to calculate the eigenvalues of the orbitals. Then, we present in some detail the tool applied, that is the metric space approach, in order to evaluate the performance of the different DFs used in this study. What is next, is the discussion of the evaluated results. Due to the large amount of the acquired data our discussion of the method performance will be based on the representative findings related to butane. Furthermore,

we added a further discussion on their performance in groups of molecules such as alkanes, aliphatic hydrocarbons, and mono or double halogen substituted hydrocarbons (i.e. ethyl- and propyl-fluoride as well as ethyl-, propyl-, n-butyl and isopropyl-chloride, and cis-1,2-dichloroethylene and 1,1-dichloroethane). Our overall remarks can be found in Conclusions section where the DFs with the most and least acceptable behavior in this type of calculations have been presented.

Computational Protocol

Calculation of Eigenvalues of Kohn-Sham Orbitals

All orbital energy eigenvalues have been calculated at the METHOD/(cc-pvtz 5d 7f[14]) (METHOD $\in$ {HF or any of the DFs mentioned in next subsection}) with Gaussian 16[15] program. These values have been scaled by using the scheme ΔSCF.[16,17] In brief, for every molecule we first optimized its geometry as to calculate the eigenvalues of the orbitals of its neutral state (E_N). Then, we performed another calculation, assuming there is not a change in the geometry when we removed 1 electron and we recalculated the eigenvalues of KS orbitals (E_{N-1}, where N=number of electrons). The energy difference E-E_{N-1} equals to vertical ionization potential (IP). Then we subtracted this value from the energy of the HOMO from the neutral state to obtain a correction factor that has to be added to all neutral eigenvalues of the KS orbitals (E_N). The present study does not focus solely on the HOMO energies but to the rest HOMO-1, HOMO-2, ... etc. For each molecule we have considered that many eigenvalues as they are experimentally available and reported in standard reference texts.[18]

Density Functionals

To facilitate the discussion we have chosen to organize the functionals considered in this work as follows:

- *Group A:* B3{LYP,P86,PW91},[5,19–24] B1{LYP, B95}[25,26] O3LYP,[27] X3LYP,[28] half and half BHandHLYP, BHandH[29]).

- *Group B:* Long range Corrected (LC) functionals, that tend to recover the inadequacy of exchange correlation functional, to describe the tails of the density: CAM-B3LYP,[30] LC-{BLYP, BP86, BPW91, ωHPBE}.[19–24,31] In addition, the following ωB97,[32] ωB97XD,[33] ωB97X,[32] have been constructed as to cure the inherent deficiency of DFs in describing the long range effects.

- *Group C:* PBE1PBE[34–36] SoGGA11-x,[37] HSEH1PBE,[38–44] OHSE2PBE,[38–44] mPW1PW91,[36] mPW91PBE, mPW3PBE, PBEh1PBE,[45] the HCTH 93, HCTH 147 and tHCTH-hyb,[46–49] TPSSh[50–52] and the BMK.[53]

- *Group D:* Minnesota functionals, developed by Truhlar's group M05,[54] M05-2X,[55] M06,[56] M06-2X,[56] M06-HF[57,58] , M06-L,[59] M08-HX,[60] M11-L,[61] M11,[62] MN12-SX,[63] N12-SX,[63] MN15,[64] MN15-L,[65] PW6B95.[66]

Metric Space and Evaluation of the Results

In the well established metric space approach,[67] we have different objects characterized by certain variables or coordinates, thus forming a set or space with dimensions equal to the number of coordinates. To calculate the distance between these objects, or in other words to define their proximity, we apply a function (that is the metric) that evaluates the coordinates of each one of the individual objects and returns a number. The reason why this approach fits well in the present study will be explained in brief. For every molecule the each one of the applied quantum chemical method is the object, and the set of objects form a space of theoretical descriptions. In the current study, each object (method) is defined by the number of eigenvalues of KS orbitals. In other words, every member is a vector and the eigenvalues are its coordinates in that space. To answer the main question of the present study that is the performance of the functionals, we have to calculate the distance between the already formed

vectors as well as between a reference vector built by the experimental orbital energies. The experimental orbital energies have been retrieved by Handbook of Chemistry and Physics.[18] To achieve this in a multidimensional space (the number of dimensions is equal to the number of coordinates which is in this case are the eigenvalues of KS orbitals) a metric function should be applied. Therefore, a generalization of the Euclidean distance to $n-$dimensions has been set as the metric of Eq. 1:

$$d_{i,j} = \sqrt{\sum_{\alpha} \frac{(Q_{i,\alpha} - Q_{j,\alpha})^2}{max_{i,j}(Q_{i,\alpha} - Q_{j,\alpha})^2}}, \tag{1}$$

In Eq. 1 $i \neq j$ and $i,\ j \in (METHODS)$, $\alpha \in$ ("orbital"), last Q is the eigenvalue that corresponds to any given α. A normalization of the obtained distances has been achieved via the presence of the denominator $max_{i,j}(Q_{i,\alpha} - Q_{j,\alpha})^2$.

Thus, the set itself along with the metric define the metric space. When the distances obtained from Eq. 1 are evaluated with the Prim algorithm[68,69] this could provide an undirected graph with the methods being the edges and the branches the respective $d_{i,j}$'s. The shortest and without loops path, often called minimum spanning tree (MST), that connects the edges provides enough information on the methods that are lying in the same neighbourhood and subsequently forming clusters. These methods are expected to perform more or less in the same manner for a given problem. These distances could be further transformed into similarities ($S_{i,j}$) by using the following formula:

$$S_{i,j} = 1 - \frac{d_{i,j}}{max_{i,j} d_{i,j}} \tag{2}$$

The existence of the denominator of Eq. 2, allows us for having values of $S_{i,j} \in [0, 1]$. It is profound that the higher the value of $S_{i,j}$ the higher the proximity between methods i and j. The already discussed approach has been introduced by Maroulis and his coworkers[70–72] and has been successfully applied in diverse studies.[73–76]

The so-called radar plot has been chosen for the visualization of the calculated similarity

values, namely $S_{METHOD,Exp}$ (Exp for experimental). In such a graphical representation, different layers correspond to different values of similarity. In the present study the closer to periphery is a given value the more similar to the experiment is, thus, the better performance of the functional that corresponds to. Therefore, the methods that are lying in deeper layers and closer to the center, are the ones with the poorest performance. Last, in addition, to calculated results and experimental data we have produced two more sets deviating 5 % and 10 % from the experimental values. These sets have been included in the search of the proximity of methods in order to address in a more direct way the meaning of the calculated similarities. That is when the relative performance of a deviation standard value (either the 5 % or 10 %) is known the other methods will find their place accordingly. Therefore, we have included in all graphs two reference lines as guides that correspond to the crucial thresholds of 5 % (green circle) and 10 % (red circle) of the reference experimental data, as they have calculated within the metric space approach.

Discussion

Given the number of the density functionals used in calculations, the number of molecules and their respective eigenvalues of KS orbitals, a large amount of calculated and evaluated data has been collected, and is available as supplementary material. What we have observed after this procedure is an almost similar performance of certain groups of methods. Therefore, it is fair to base our discussion on the performance of groups of DFs on the representative data obtained for butane. For this reason we have included a graphical representation of the similarities of DFs towards experimental data ($S_{METHOD,Exp}$) in Fig. 1. In addition, we took advantage of the calculated $d_{i,j}$'s and constructed the MST (see Fig. 2) to obtain insights on clusters of methods of similar performance. Since, the other leg of the present study concerns the performance of DFs towards groups of molecules, we based our discussion on the graphical representation of the similarity values between DFs and experimental data

(see Fig. 3, 4, 5, 6, 7). The groups of molecules have been constructed by having in mind that we would like to gain insights on the subject by examining the effect of saturation (e.g. ethane vs ethylene, propane vs propene, butane vs 2-butene etc). Furthermore, to study the effect of halogen substitution such as fluoride and chloride we studied ethyl-, propyl- fluoride and chloride, butyl- chloride and isopropyl-chloride. In addition, we are presenting results of calculations on methanol and ethanol, whereas more results of compounds containing -SH and -NH_2, can be found in supplementary material.

Group A: The well known Becke's B3 hybrid scheme when combined with the correlation functionals LYP and PW91 (resulting to B3LYP and B3PW91 in Gaussian,[15] respectively), does not produce results in close similarity with the set of nine experimental data we have considered. The relative values have been tabulated in Table 1. Whereas, their relative performance has been depicted in Fig. 1, where the green and red lines have been used as borders to separate the functionals that are producing eigenvalues of KS orbitals that are by less than 5 % or 10 %, corresponding to similarity values of 0.72 and 0.44, respectively, far from the reference ones. As it can be seen in this figure, both functionals are in between the red and green lines with similarity values of 0.7. On the other hand, the combination with P86 correlation functional, resulting to B3P86 approximation, gave $S_{B3P86,Exp}$=0.88, thus clearly, outperforms the other two as it can be seen in Table 1. In the same table one would find the results of the X3 scheme along with the LYP correlation functional (X3LYP functional) with a $S_{X3LYP,Exp}$=0.7, that mimics the performance of B3LYP and B3PW91 methods. Even worse is the performance of the O3LYP functional, that lies closer to the red line, given its $S_{O3LYP,Exp}$=0.58. Among the first batch of "hybrid" functionals the O3LYP seem to be the less effective in diverse calculations[73–76] (the observed inadequacy of the B3 scheme is further manifested by the fact that the mPW1PW91 functional produces results characterized by large similarity to reference values). Another "hybrid" approach, that is also based on the philosophy introduced by Becke, has been introduced via the B1 scheme (1 is for one parameter). This part has been combined with both LYP and B95

leading to B1LYP and B1B95 functionals, respectively. However, neither of them seem to be able to produce highly ranked results as it can be seen in both Fig. 1 and the respective $S_{B1LYP,Exp}$=0.69 and $S_{B1B95,Exp}$=0.70 values. Noteworthy is the performance of the *Gaussian 16* modified version of the so called "half and half" functionals (BHandHLYP and BHandH): $S_{BHandHLYP,Exp}$=0.89 and $S_{BHand,Exp}$=0.86. It can be said that they are well performers, in general, with two noticeable downfalls in the case of Ethyl Chloride and 2-Chloroethanol. The last member of the "hybrids" is the prominent[77] APFD functional that has been also implemented in our calculations, however its performance should be characterized as poor, as the value $S_{APFD,Exp}$=0.72 reveals. Among the functionals of this group the B3P86 seems to be adequate for calculation of eigenvalues of orbitals.

Group B: The so called "long range correction" scheme has been applied to BLYP, BP86, BPW91 and ωHPBE functionals (respective values are in Table 2). The most affected seem to be the BP86 since it produces results that are (constantly) well below the other three: $S_{LC-BLYP,Exp}$=0.85, $S_{LC-BP86,Exp}$=0.78 and $S_{LC-BPW91,Exp}$=0.82. Their performance in absolute values has been tabulated in Table 2. On the contrary the LC-ωHPBE is the leading one since it is most of the times quite close to experimental results, as it is in the case of butane with a $S_{LC\omega HPBE,Exp}$=0.89. Some other members, like ωB97, B97X and ωB97XD most of the times are also among the best performing DFs. What is worth noting, and can be easily observed in all graphs, is the fact that when the latter group is on the top the group of LC-B{LYP,P86,PW91} comes after and vice versa that is when the LC-B{LYP,P86,PW91} group goes to the top the other follows from a distance.

The most prominent representative of **Group C** is the PBE1PBE functional, that mixes PBE and Hartree-Fock energy. This group contains PBE1PBE ($S_{HSEH1PBE,Exp}$ = 0.73), HSEH1PBE ($S_{HSEH1PBE,Exp}$ = 0.72), OHSE2PBE ($S_{OHSE2PBE,Exp}$ = 0.82), PBEh1PBE ($S_{PBEh1PBE,Exp}$ = 0.73), mPW91PBE ($S_{mPW91PBE,Exp}$ = 0.73), mPW3PBE ($S_{mPW3PBE,Exp}$ = 0.70) and LC-ωHPBE, as well. The results obtained (see Table 3) with this large group are most of the times on the region of the less than 5 % difference from the reference value

as it can be seen in Table 3. Among them the LC-ωHPBE that combines the *long range correction* scheme along with the *GG* approximation is the one that ranks at the top of the similarity scale. Of the same quality is the SOGGA11-x functional, that scores a value of $S_{SOGGA11x,Exp}$=0.86. Last, two distinct subsets of this group are the HCTH family (HCTH93, HCTH147, tHCTHhyb) and the TPSSh, that is *meta*-GGA, with both sets to lie very low in the ranking list and in between the red and green lines, as it can be seen in the Fig. 1. It is worth noting that the improved version (by including the term of the kinetic energy density plus a modification on the value of the exact mixing coefficient) of the HCTH functionals that is the BMK functional clearly manages to substantially improve the obtained results with $S_{BMK,Exp}$=0.85. Thus, it is the latter functional along with SOGGA11-x and the LC-ωHPBE that are the leaders in the race of good performers. However, after taking into account their overall performance, it is fair to propose only LC-ωHPBE for this type of calculations.

The **Group D**, containing some Minnesota Functionals, is another group of DFs tested in the present study. Truhlar and co-workers have produced a vast number of density functionals characterized by extensive parametrization, while the optimized parameters have been produced upon fitting on more sophisticated data sets. The fruits of this effort, among others, have been the M05 and M05-2X, M06, M06-2X and M06-HF, M08-HX, M11-L, M11, MN15-L, MN12-SX, MN15 and N12-SX functionals. Moreover they have experimentalized with the amount of the "optimal" amount of HF that a functional should contain. That is the 2X corresponds to an increment of the percentage of the HF that is included in the exchange part of the functional. In practice this has been applied in M05 and M05-2X (from 28% to 56%, respectively) as well as in M06 and M06-2X (from 27 % to 54%, respectively), functionals. This choice sufficiently improves the quality of the obtained results as it can be seen in the similarity values: $S_{M05,Exp}$=0.69 and $S_{M05-2X,Exp}$=0.89, $S_{M06,Exp}$=0.72 and $S_{M06-2X,Exp}$=0.89. This is also proven by the results included in Table 4. However, it is not to be said that the more HF it is included the better the obtained results, since the use of the

M06-HF, that includes 100 % of the HF, resulted to poorer performance ($S_{M06-HF,Exp}$=0.56). The MN15 is a hybrid functional whereas MN15-L is a local one, with the first of the them to produce better results as the values $S_{MN15,Exp}$=0.81 and $S_{MN15L,Exp}$=0.67 clearly show. Among the other members M08-HX and M11 are also capable of producing results that lie close to experimental findings: $S_{M08-HX,Exp}$=0.89 and $S_{M11,Exp}$=0.89. Therefore, it can be expected that M05-2X, M06-2X, M08-HX and M11 DFs could provide reliable results.

Before discussing the performance of methods in groups of molecules we present in Fig. 2 the way methods cluster when they exhibit the similar performance. For example the methods that seem to lie on the vicinity of experimental values are LC-ωHPBE, M05-2X, ωB97, BhandHLYP, M06-2X, M08-HX, LC-ωPBE and M11. Close to this cluster we can find two smaller neighbourhoods: one consists of ωB97X, SoGGA11-x, BMK and CAM-B3LYP, and the other one with OHSE2PBE, MN15 and ωB97XD. Even further from the reference data is the cluster that contains PW6B95, mPW1PW91, mPW1PBE, PBEh1PBE, PBE1PBE, HSEH1PBE, APFD, N12-SX, mPW3PBE, B3PW91, X3LYP, B1LYP, M05, MN15-L, tHCTHhyb and TPSSh. The O3LYP, M06-L, tHCTH and HCTH147 functionals form the last cluster lying at the edges. There are also functionals that are not grouped and they most of the time lie aside of the larger clusters.

Our findings are in agreement with what has been found in existing studies, however dealing only with the HOMO and LUMO KS energy eigenvalues. For example, the adequate performance of LC-ωPBE has been also observed in the studies by Vydrov and Scuseria[6] and by Sun et al[8] where they concluded that in general the LC-DFT perform well. Further studies by Kang et al[12] and Brédas et al[78] who reported on electron affinities and ionization energies of molecular crystals, respectively, also came to the same conclusion. A similar study by Rayne and Forest[79] on short- through long-chain [n]acenes and [n]phenacenes revealed the acceptable performance of M06-2X and MN12-SX functionals, as well.

The above presented analysis is based on the findings on a particular molecule, that is, butane. However, similar results have been obtained for the rest of the members of the

set of molecules under study. This is manifested in multiple figures (see Fig. 3, 4, 5 and 6) where $S_{METHOD,exp}$ values have been depicted to support, on the one hand, the already discussed findings and on the other to assist the discussion that follows, where we examine the performance of functionals in groups containing homologue compounds.

After having discussed the performance of DFs in general it is of some importance to focus on their performance in respect to groups of molecules. Starting with ethane, propane and butane (see Fig. 3) one can easily recognize the large dispersion of the relative performances of the DFs. In addition, it seems that the convergence of the calculated values to the reference ones is benefited by the increment of the carbon chain, at least for these first members of n-alkanes group. The results for the unsaturated compounds of the same group have been depicted in Fig. 4. The information that can be retrieved from these figures is that the smaller the compound the less the dispersion of the performance of the density functionals. We further investigated the subject by observing the sequence propane, propene and propyne (see Fig. 5). What we found is that for this group the less the saturation the better the performance, meaning that $S_{METHOD,Exp}$ values are increasing in the order single, double and triple bond of a 3 atom carbon chain. From all the above it is obvious that we can't conclude to an overall finding.

The effect of the substitution of one hydrogen of the chain with either fluoride or chloride has been also studied. The pictures from ethyl fluoride and n-propyl fluoride are both characterized from a large dispersion of similarity values. A larger set of substituted hydrocarbons containing chloride has been tested. The findings suggest that from a rather chaotic picture in the case of ethyl chloride we are moving gradually to a highly ordered picture in the case of n-butyl chloride through propyl-, isopropyl-chloride, as well as cis-1,2-dichloroethylene (see Fig. 6).

Rather smooth is the convergence of DFs to reference values in the case of methanol and ethanol (see Fig. 7) as well as mercaptan and n-propyl thiol. However, an abrupt change of this picture is observed when chloride or -NH_2 groups are added to these systems, as in the

case of ethanol chloride and 2-amino-ethanol.

Conclusion

We have collected a significant amount of results related to computed DFT eigenvalues of orbitals of a wide range of simple but reference chemical moieties for which experimental estimates are available via UV-VIS-PES. Our findings clearly suggest that an amount of Hartree-Fock exchange correlation is mandatory. Most of the functionals that follow the "hybrid" scheme are in fair agreement with the reference values. However, when the Hartree-Fock portion is pronounced, as in the case of the M06-HF, the opposite effect is delivered. The quality of results seems to be negatively affected, as well, when the B3 and B1 terms are chosen. Such an effect has been observed also in the case of B3LYP and B3PW91 methods, whereas a better performance is revealed when the B3P86 functional has been used. The long-range-corrected functionals produce results characterized of better quality. This is depicted in the performance of both ωB97 and LC-ωHPBE, which seem better performers in the calculation of ground state eigenvalues of orbitals, than other long range corrected schemes applied in the present study. The latter along with the BMK are the ones that also ranked high in the list of the reliable functionals among the DFs that further include the generalized gradient correction approximation. Last, M05-2X, M06-2X and M08-HX functionals are also leading the race of good performers.

In terms of bonding features we found that for saturated hydrocarbons the larger the carbon chain the better the performance of DFs. The inverse has been observed in the case of their unsaturated analogues. The effect of saturation has been further studied in the case of a 3 carbon chain containing single, double and triple bonds (propane, propene and propyne, respectively) with functionals to perform better in this order. Quite descriptive is the effect of chloride substituted hydrocarbons. In this group we have seen that the larger the carbon chain the better the behaviour. Similar findings have been extracted in the OH and SH

substituted ethyl and propyl hydrocarbons. However, when both OH and Cl or OH and NH_2 are present, the behaviour of the DF methods could not be characterized as acceptable.

Authors Declarations

The authors have no conflicts to disclose.

Data Availability

The data that support the findings of this study are available from the corresponding author upon reasonable request.

References

(1) Nugroho, A. E.; Morita, H. Computationally-assisted discovery and structure elucidation of natural products. *J. Nat. Med.* **2019**, *73*, 687–695.

(2) Borges, R. M.; Colby, S. M.; Das, S.; Edison, A. S.; Fiehn, O.; Kind, T.; Lee, J.; Merrill, A. T.; Merz, K. M.; Metz, T. O.; Nunez, J. R.; Tantillo, D. J.; Wang, L.-P.; S.Wang,; Renslow, R. S. Quantum chemistry Calculations for Metabolomics. *Chem. Rev.* **2021**, *121*, 5633–5670.

(3) Ozaki, Y.; Be, K. B.; Morisawa, Y.; Yamamoto, S.; Tanabe, I.; Huck, C. W.; Hofer, T. S. Advances, Challenges and Perspectives of Quantum Chemical Approaches in Molecular Spectroscopy of the Condensed Phase. *Chem. Soc. Rev.* **2021**, *50*, 10917–10954.

(4) Zhan, C.-G.; Nichols, J. A.; Dixon, D. A. Ionization Potential, Electron Affinity, Electronegativity, Hardness, and Electron Excitation Energy: Molecular Properties from Density Functional Theory Orbital Energies. *J. Phys. Chem. A* **2003**, *107*, 4184–4195.

(5) Becke, A. D. Density-functional thermochemistry. III. The role of exact exchange. *J. Chem. Phys.* **1993**, *98*, 5648–5652.

(6) Vydrov, O. A.; Scuseria, G. E. Assessment of a long-range corrected hybrid functional. *J. Chem. Phys.* **2006**, *125*, 234100.

(7) Henderson, T. M.; Izmaylov, A. F.; Scalmani, G.; ; Scuseria, G. E. Can short-range hybrids describe long-range-dependent properties? *J. Chem. Phys.* **2009**, *131*, 044108.

(8) Sun, H.; Zhang, S.; Sun, Z. Applicability of optimal functional tuning in density functional calculations of ionization potentials and electron affinities of adeninethymine nucleobase pairs and clusters. *Phys. Chem. Chem. Phys.* **2015**, *17*, 4337–4345.

(9) Knight, J. W.; Wang, X.; Gallandi, L.; Dolgounitcheva, O.; Ren, X.; Ortiz, J. V.; Rinke, P.; Körzdörfer, T.; Marom, N. Accurate Ionization Potentials and Electron Affinities of Acceptor Molecules III: A Benchmark of GW Methods. *J. Chem. Theory Comput.* **2016**, 615–626.

(10) Hedin, L. New method for calculating the one-particle green's function with application to the electron-gas problem. *Phys. Rev.* **1965**, *139*, A796.

(11) Aryasetiawan, F.; Gunnarsson, O. New method for calculating the one-particle green's function with application to the electron-gas problem. *Rep. Prog. Phys.* **1998**, *61*, 237.

(12) Kang, Y.; Jeon, S. H.; Cho, Y.; Han, S. *Ab initio* calculation of ionization potential and electron affinity in solid-state organic semiconductors. *Phys. Rev. B* **2016**, *93*, 035131.

(13) Kirchner-Hall, N. E.; Zhao, W.; Xiong, Y.; Timrov, I.; Dabo, I. Extensive Benchmarking of DFT+U Calculations for Predicting Band Gaps. *Appl. Sci.* **2021**, 2395.

(14) Dunning, T. H. Gaussian basis sets for use in correlated molecular calculations. I. The atoms boron through neon and hydrogen. *J. Chem. Phys.* **1989**, *90*, 1007–1023.

(15) Frisch, M. J. et al. Gaussian16 Revision C.01. 2016; Gaussian Inc. Wallingford CT.

(16) Bagus, P. S. Self-Consistent-Field Wave Functions for Hole States of Some Ne-Like and Ar-Like Ions. *Phys. Rev. A* **1965**, *139*, 619–634.

(17) Moser, C.; Nesbet, R. K.; G., V. A correlation energy calculation of the 1s hole state in neon. *Chem. Phys. Lett.* **1971**, *12*, 230–232.

(18) Stone, A. J., Ed. *Handbook Handbook of Chemistry and Physics*, 11th ed.; Oxford University Press: UK, 1997.

(19) Perdew, J. P. Density-functional approximation for the correlation energy of the inhomogeneous electron gas. *Phys. Rev. B* **1986**, *33*, 8822–8824.

(20) Perdew, J. P. In *in Electronic Structure of Solids*, 11th ed.; Ziesche, P., Eschrig, H., Eds.; Akademie Verlag: Berlin, 1991.

(21) Perdew, J. P.; Chevary, J. A.; Vosko, S. H.; Jackson, K. A.; Pederson, M. R.; Singh, D. J.; Fiolhais, C. Atoms, molecules, solids, and surfaces: Applications of the generalized gradient approximation for exchange and correlation. *Phys. Rev. B* **1992**, *46*, 6671–6687.

(22) Perdew, J. P.; Chevary, J. A.; Vosko, S. H.; Jackson, K. A.; Pederson, M. R.; Singh, D. J.; Fiolhais, C. Erratum: Atoms, molecules, solids, and surfaces: Applications of the generalized gradient approximation for exchange and correlation. *Phys. Rev. B* **1993**, *48*, 4978.

(23) Perdew, J. P.; Burke, K.; Wang, Y. Generalized gradient approximation for the exchange-correlation hole of a many-electron system. *Phys. Rev. B* **1996**, *54*, 16533–16539.

(24) Burke, K.; Perdew, J. P.; Wang, Y. In *in Electronic Density Functional Theory: Recent*

Progress and New Directions; Dobson, J. F., Vignale, G., Das, M. P., Eds.; Akademie Verlag: Plenum, 1998.

(25) Adamo, C.; Barone, V. Toward Reliable Adiabatic Connection Models Free From Adjustable Parameters. *Chem. Phys. Lett.* **1997**, *274*, 242–250.

(26) Becke, A. D. Density-Functional Thermochemistry. IV. A New Dynamical Correlation Functional and Implications for Exact-Exchange Mixing. *J. Chem. Phys.* **1996**, *104*, 1040–1046.

(27) Cohen, A. J.; Handy, N. C. Dynamic correlation. *Mol. Phys.* **2001**, *99*, 607–615.

(28) Xu X.,; Goddard W. A, III, The X3LYP extended density functional for accurate descriptions of nonbond interactions, spin states, and thermochemical properties. *Proc. Natl. Acad. Sci. USA* **2004**, *101*, 2673–2677.

(29) Becke, A. D. A new mixing of Hartree-Fock and local density-functional theories. *J. Chem. Phys.* **1993**, *98*, 1372–1377.

(30) Yanai, T.; Tew, D.; Handy, N. A new hybrid exchange-correlation functional using the Coulomb-attenuating method (CAM-B3LYP). *Chem. Phys. Lett.* **2004**, *393*, 51–57.

(31) Iikura, H.; Tsuneda, T.; Yanai, T.; Hirao, K. Long-range correction scheme for generalized-gradient-approximation exchange functionals. *J. Chem. Phys.* **1999**, *115*, 3540–3544.

(32) Chai, J.-D.; Head-Gordon, M. Systematic optimization of long-range corrected hybrid density functionals. *J. Chem. Phys.* **2008**, *128*, 084106.

(33) Chai, J.-D.; Head-Gordon, M. Long-range corrected hybrid density functionals with damped atom-atom dispersion corrections. *Phys. Chem. Chem. Phys.* **2008**, *10*, 6615–6620.

(34) Perdew, J. P.; Burke, K.; Ernzerhof, M. Generalized gradient approximation made simple. *Phys. Rev. Lett.* **1996**, *77*, 3865–3868.

(35) Perdew, J. P.; Burke, K.; Ernzerhof, M. Errata: Generalized gradient approximation made simple. *Phys. Rev. Lett.* **1997**, *78*, 1396.

(36) Adamo, C.; Barone, V. Toward reliable density functional methods without adjustable parameters: The PBE0 model. *J. Chem. Phys.* **1999**, *110*, 6158–6169.

(37) Peverati, R.; Truhlar, D. G. A global hybrid generalized gradient approximation to the exchange-correlation functional that satisfies the second-order density-gradient constraint and has broad applicability in chemistry. *J. Chem. Phys.* **2011**, *135*, 191102.

(38) Heyd, J.; Scuseria, G. E. Hybrid functionals based on a screened Coulomb potential. *J. Chem. Phys.* **2003**, *118*, 8207–8215.

(39) Heyd, J.; Scuseria, G. E. Assessment and validation of a screened Coulomb hybrid density functional. *J. Chem. Phys.* **2004**, *120*, 7274–7280.

(40) Heyd, J.; Scuseria, G. E. Efficient hybrid density functional calculations in solids: The HS-Ernzerhof screened Coulomb hybrid functional. *J. Chem. Phys.* **2004**, *121*, 1187–1192.

(41) Heyd, J.; Peralta, J. E.; Scuseria, G. E.; Martin, R. L. Energy band gaps and lattice parameters evaluated with the Heyd-Scuseria-Ernzerhof screened hybrid functional. *J. Chem. Phys.* **2005**, *123*, 174101.

(42) Heyd, J.; Scuseria, G. E. Erratum: Hybrid functionals based on a screened Coulomb potential. *J. Chem. Phys.* **2006**, *124*, 219906.

(43) Izmaylov, A. F.; Scuseria, G. E.; Frisch, M. J. Efficient evaluation of short-range Hartree-Fock exchange in large molecules and periodic systems. *J. Chem. Phys.* **2006**, *125*, 104103.

(44) Krukau, A. V.; Vydrov, O. A.; Izmaylov, A. F.; Scuseria, G. E. Influence of the exchange screening parameter on the performance of screened hybrid functionals. *J. Chem. Phys.* **2006**, *125*, 224106.

(45) Ernzerhof, M.; Perdew, J. P. Generalized gradient approximation to the angle- and system-averaged exchange hole. *J. Chem. Phys.* **1998**, *109*, 3313–3320.

(46) Hamprecht, F. A.; Cohen, A.; Tozer, D. J.; Handy, N. C. Development and assessment of new exchange-correlation functionals. *J. Chem. Phys.* **1998**, *109*, 6264–6271.

(47) Boese, A. D.; Doltsinis, N. L.; Handy, N. C.; Sprik, M. New generalized gradient approximation functionals. *J. Chem. Phys.* **2000**, *112*, 1670–1678.

(48) Boese, A. D.; Handy, N. C. A new parametrization of exchange-correlation generalized gradient approximation functionals. *J. Chem. Phys.* **2001**, *114*, 5497–5503.

(49) Boese, A. D.; Handy, N. C. New exchange-correlation density functionals: The role of the kinetic-energy density. *J. Chem. Phys.* **2002**, *116*, 9559–9569.

(50) Tao, J. M.; Perdew, J. P.; Staroverov, V. N.; Scuseria, G. E. Climbing the density functional ladder: Nonempirical meta-generalized gradient approximation designed for molecules and solids. *Phys. Rev. Lett.* **2003**, *91*, 146401.

(51) Staroverov, V. N.; Scuseria, G. E.; Tao, J.; Perdew, J. P. Comparative assessment of a new nonempirical density functional: Molecules and hydrogen-bonded complexes. *J. Chem. Phys.* **2003**, *119*, 12129.

(52) Staroverov, V. N.; Scuseria, G. E.; Tao, J.; Perdew, J. P. (Erratum): Comparative assessment of a new non empirical density functional: Molecules and hydrogen-bonded complexes. *J. Chem. Phys.* **2004**, *121*, 11507.

(53) Boese, A. D.; Martin, J. M. L. Development of Density Functionals for Thermochemical Kinetics. *J. Chem. Phys.* **2004**, *121*, 3405–3416.

(54) Zhao, Y.; Schultz, N. E.; Truhlar, D. G. Exchange-correlation functional with broad accuracy for metallic and nonmetallic compounds, kinetics, and noncovalent interactions. *J. Chem. Phys.* **2005**, *123*, 161103.

(55) Zhao, Y.; Schultz, N. E.; Truhlar, D. G. Design of density functionals by combining the method of constraint satisfaction with parametrization for thermochemistry, thermochemical kinetics, and noncovalent interactions. *J. Chem. Theory Comput.* **2006**, *2*, 364–382.

(56) Zhao, Y.; Truhlar, D. G. The M06 suite of density functionals for main group thermochemistry, thermochemical kinetics, noncovalent interactions, excited states, and transition elements: two new functionals and systematic testing of four M06-class functionals and 12 other functionals. *Theor. Chem. Acc.* **2008**, *120*, 215–241.

(57) Zhao, Y.; Truhlar, D. G. Comparative DFT study of van der Waals complexes: Rare-gas dimers, alkaline-earth dimers, zinc dimer, and zinc-rare-gas dimers. *J. Phys. Chem.* **2006**, *110*, 5121–5129.

(58) Zhao, Y.; Truhlar, D. G. Density Functional for Spectroscopy: No Long-Range Self-Interaction Error, Good Performance for Rydberg and Charge-Transfer States, and Better Performance on Average than B3LYP for Ground States. *J. Phys. Chem. A* **2006**, *110*, 13126–13130.

(59) Zhao, Y.; Truhlar, D. G. A new local density functional for main-group thermochemistry, transition metal bonding, thermochemical kinetics, and noncovalent interactions. *J. Chem. Phys.* **2006**, *125*, 194101.

(60) Zhao, Y.; Truhlar, D. G. Exploring the Limit of Accuracy of the Global Hybrid Meta Density Functional for Main-Group Thermochemistry, Kinetics, and Noncovalent Interactions. *J. Chem. Theory Comput.* **2008**, *4*, 1849–1868.

(61) Peverati, R.; Truhlar, D. G. M11-L: A Local Density Functional That Provides Improved Accuracy for Electronic Structure Calculations in Chemistry and Physics. *J. Phys. Chem. Lett.* **2012**, *3*, 117–124.

(62) Peverati, R.; Truhlar, D. G. Improving the Accuracy of Hybrid Meta-GGA Density Functionals by Range Separation. *J. Phys. Chem. Lett.* **2011**, *2*, 2810–2817.

(63) Peverati, R.; Truhlar, D. G. Screened-exchange density functionals with broad accuracy for chemistry and solid state physics. *Phys. Chem. Chem. Phys.* **2012**, *14*, 16187.

(64) Yu, H. S.; He, X.; Li, S. L.; Truhlar, D. G. MN15: A Kohn-Sham Global-Hybrid Exchange-Correlation Density Functional with Broad Accuracy for Multi-Reference and Single-Reference Systems and Noncovalent Interactions. *Chem. Sci.* **2016**, *7*, 5032–5051.

(65) Yu, H. S.; He, X.; Truhlar, D. G. MN15-L: A New Local Exchange-Correlation Functional for KohnSham Density Functional Theory with Broad Accuracy for Atoms, Molecules, and Solids. *J. Chem. Theory Comput.* **2016**, *12*, 1280–1293.

(66) Zhao, Y.; Truhlar, D. G. Design of Density Functionals That Are Broadly Accurate for Thermochemistry, Thermochemical Kinetics, and Nonbonded Interactions. *J. Phys. Chem. A* **2005**, *109*, 5656–5667.

(67) Similarity Search: The Metric Space Approach. **2006**,

(68) Jarník, V. O jistém problému minimálním. *Práce Moravské Pírodovdecké Spolenosti* **1930**, *6*, 57–63.

(69) Prim, R. C. Shortest connection networks and some generalizations. *Bell Syst. Tech. J.* **1957**, *36*, 1389–1401.

(70) Maroulis, G.; Sana, M.; Leroy, G. Molecular properties and basis set quality: An approach based on information theory. *Int. J. Quant. Chem.* **1981**, *19*, 43–60.

(71) Maroulis, G. Control over theoretical descriptions of atoms and molecules. An information theoretic approach to the automatic classification and systematic improvement of approximate wave functions. *Int. J. Quant. Chem.* **1988**, *34*, 185–190.

(72) Maroulis, G. Evaluating the performance of correlated methods in molecular property calculations: Pattern recognition and clustering in spaces of theoretical descriptions. *Int. J. Quant. Chem.* **1995**, *55*, 173–180.

(73) Maroulis, G.; Karamanis, P. Comparison of conventional ab initio and DFT quantum chemical methods. The electric moments and (hyper)polarizability of H-C=C-C=C-H as a test case. *MATCH Commun. Math. Comput. Chem.* **2005**, *53*, 269–282.

(74) Christodouleas, C. S.; Xenides, D.; Simos, T. E. Trends of the bonding effect on the performance of DFT methods in electric properties calculations: A pattern recognition and metric space approach on some XY_2 (X = O, S and Y = H, O, F, S, Cl) molecules. *J. Comp. Chem.* **2010**, *31*, 412–420.

(75) Xenides, D.; Karamanis, P.; Pouchan, C. A critical analysis of the performance of new generation functionals on the calculation of the (hyper) polarizabilities of clusters of varying stoichiometry: Test case the Si_mGe_n (m + n = 7, n = 0-7) clusters. *Chem. Phys. Lett.* **2010**, *498*, 134–139.

(76) Xenides, D.; Fostiropoulou, D.; Vlachos, D. A Metric Space Approach on the Molecular vs. Chemical Similarity of Some Analgesic and Euphoric Compounds. *MATCH Commun. Math. Comput. Chem.* **2020**, *83*, 261–284.

(77) Austin, A.; Petersson, G.; Frisch, M. J.; Dobek, F. J.; Scalmani, G.; Throssell, K. A density functional with spherical atom dispersion terms. *J. Chem. Theory Comput.* **2012**, *8*, 4989–5007.

(78) Sun, H.; Ryno, S.; Zhong, C.; Ravva, M. K.; Sun, Z.; Körzdörfer, T.; Brédas, J.-L. Ionization Energies, Electron Affinities, and Polarization Energies of Organic Molecular

Crystals: Quantitative Estimations from a Polarizable Continuum Model (PCM)-Tuned Range-Separated Density Functional Approach. *J. Chem. Theory Comput.* **2016**, 2906–2915.

(79) Rayne, S.; Forest, K. Benchmarking semiempirical, Hartree-Fock, DFT, and MP2 methods against the ionization energies and electron affinities of short- through long-chain [n]acenes and [n]phenacenes. *Can. J. Chem.* **2016**, *94*, 251–258.

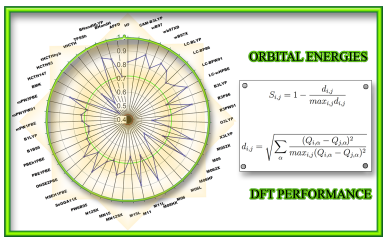
ORBITAL ENERGIES
$S_{i,j} = 1 - \frac{d_{i,j}}{max_{i,j} d_{i,j}}$
$d_{i,j} = \sqrt{\sum_{\alpha} \frac{(Q_{i\alpha} - Q_{j\alpha})^2}{max_{i,j}(Q_{i\alpha} - Q_{j\alpha})^2}}$
DFT PERFORMANCE

Cover image

Table 1: Differences between experimental and calculated orbital energies of butane, defined as $E_{exp} - E_{METHOD}$ of the *Group A* class (in parenthesis are the calculated energies)

HOMO-n, n=	B3LYP	B3P86	B3PW91	B1B95	B1LYP	X3LYP	O3LYP	BhandH	BhandHLYP
0	0.11	0.61	0.04	0.02	0.07	0.10	-0.21	0.23	0.58
	(-11.20)	(-11.70)	(-11.13)	(-11.11)	(-11.16)	(-11.19)	(-10.88)	(-11.32)	(-11.67)
1	-0.45	0.10	-0.47	-0.52	-0.50	-0.46	-0.72	-0.20	0.04
	(-11.21)	(-11.76)	(-11.19)	(-11.14)	(-11.16)	(-11.20)	(-10.94)	(-11.46)	(-11.70)
2	-0.78	-0.20	-0.78	-0.82	-0.84	-0.79	-1.05	-0.42	-0.30
	(-11.52)	(-12.10)	(-11.52)	(-11.48)	(-11.46)	(-11.51)	(-11.25)	(-11.88)	(-12.00)
3	-0.77	-0.26	-0.82	-0.84	-0.80	-0.79	-1.08	-0.57	-0.21
	(-11.97)	(-12.48)	(-11.92)	(-11.90)	(-11.94)	(-11.95)	(-11.66)	(-12.17)	(-12.53)
4	-0.74	-0.19	-0.75	-0.77	-0.77	-0.75	-1.04	-0.40	-0.14
	(-12.46)	(-13.01)	(-12.45)	(-12.43)	(-12.43)	(-12.45)	(-12.16)	(-12.80)	(-13.06)
5	-0.59	-0.03	-0.60	-0.58	-0.60	-0.59	-0.93	-0.09	0.14
	(-13.61)	(-14.17)	(-13.60)	(-13.62)	(-13.60)	(-13.61)	(-13.27)	(-14.11)	(-14.34)
6	-0.76	-0.13	-0.72	-0.69	-0.78	-0.75	-1.08	-0.06	-0.02
	(-13.83)	(-14.46)	(-13.87)	(-13.90)	(-13.81)	(-13.84)	(-13.51)	(-14.53)	(-14.57)
7	-0.98	-0.37	-0.95	-0.92	-0.99	-0.97	-1.30	-0.33	-0.21
	(-14.02)	(-14.63)	(-14.05)	(-14.08)	(-14.01)	(-14.03)	(-13.70)	(-14.67)	(-14.79)
8	-0.82	-0.21	-0.80	-0.72	-0.81	-0.80	-1.20	0.00	0.09
	(-15.17)	(-15.78)	(-15.19)	(-15.27)	(-15.18)	(-15.19)	(-14.79)	(-15.99)	(-16.08)

Table 2: Differences between experimental and calculated orbital energies of butane, defined as $E_{exp} - E_{METHOD}$ of the *Group B* class (in parenthesis are the calculated energies)

HOMO-n, n=	LC-ωPBE	LC-ωHPBE	CAM-B3LYP	LC-BLYP	LC-BP86	LC-BPW91	ωB97D	ωB97XD
0	0.60	0.60	0.39	0.72	0.84	0.76	0.59	0.29
	(-11.69)	(-11.69)	(-11.48)	(-11.81)	(-11.93)	(-11.85)	(-11.68)	(-11.38)
1	0.08	0.08	-0.15	0.23	0.41	0.32	0.02	-0.27
	(-11.74)	(-11.74)	(-11.51)	(-11.89)	(-12.07)	(-11.98)	(-11.68)	(-11.39)
2	-0.20	-0.20	-0.45	-0.01	0.21	0.10	-0.26	-0.57
	(-12.10)	(-12.10)	(-11.85)	(-12.29)	(-12.51)	(-12.40)	(-12.04)	(-11.73)
3	-0.18	-0.18	-0.45	-0.06	0.08	0.01	-0.23	-0.55
	(-12.56)	(-12.56)	(-12.29)	(-12.68)	(-12.82)	(-12.75)	(-12.51)	(-12.19)
4	-0.06	-0.06	-0.37	0.09	0.27	0.19	-0.13	-0.48
	(-13.14)	(-13.14)	(-12.83)	(-13.29)	(-13.47)	(-13.39)	(-13.07)	(-12.72)
5	0.25	0.25	-0.14	0.45	0.65	0.57	0.18	-0.25
	(-14.45)	(-14.45)	(-14.06)	(-14.65)	(-14.85)	(-14.77)	(-14.38)	(-13.95)
6	0.16	0.16	-0.26	0.39	0.67	0.57	0.07	-0.38
	(-14.75)	(-14.75)	(-14.33)	(-14.98)	(-15.26)	(-15.16)	(-14.66)	(-14.21)
7	-0.05	-0.05	-0.48	0.17	0.42	0.33	-0.15	-0.60
	(-14.95)	(-14.95)	(-14.52)	(-15.17)	(-15.42)	(-15.33)	(-14.85)	(-14.40)
8	0.28	0.28	-0.23	0.56	0.82	0.73	0.19	-0.36
	(-16.27)	(-16.27)	(-15.76)	(-16.55)	(-16.81)	(-16.72)	(-16.18)	(-15.63)

Table 3: Differences between experimental and calculated orbital energies of butane, defined as $E_{exp} - E_{METHOD}$ of the *Group C* class (in parenthesis are the calculated energies)

HOMO-n, n=	PBE1PBE	PBEH1PBE	SOGGA11-x	HSEH1PBE	OHSEH2PBE	HCTH93	HCTH147	tHCTHhyb	TPSSH	mPW1PBE	mPW3PBE	BMK	APFD	mPW1PW91	mPW91PBE
0	0.07	0.08	0.47	0.06	0.33	-0.42	-0.27	0.03	-0.05	0.09	0.04	0.38	0.07	0.12	0.09
	(-11.16)	(-11.17)	(-11.56)	(-11.15)	(-11.42)	(-10.67)	(-10.82)	(-11.12)	(-11.04)	(-11.18)	(-11.13)	(-11.47)	(-11.16)	(-11.21)	(-11.18)
1	-0.43	-0.42	-0.10	-0.44	-0.17	-0.91	-0.76	-0.52	-0.55	-0.42	-0.46	-0.06	-0.44	-0.39	-0.42
	(-11.23)	-11.24)	-11.56)	(-11.22)	(-11.49)	(-10.75)	(-10.90)	(-11.14)	(-11.11)	(-11.24)	(-11.20)	-(11.60)	(-11.22)	(-11.27)	(-11.24)
2	-0.72	-0.71	-0.41	-0.73	-0.47	-1.24	-1.09	-0.86	-0.96	-0.72	-0.77	-0.50	-0.74	-0.70	-0.72
	(-11.58)	(-11.59)	(-11.89)	(-11.57)	(-11.83)	(-11.06)	(-11.21)	(-11.44)	(-11.34)	(-11.58)	(-11.53)	(-11.80)	(-11.56)	(-11.60)	(-11.58)
3	-0.78	-0.77	-0.37	-0.80	-0.52	-1.31	-1.18	-0.86	-0.89	-0.76	-0.82	-0.35	-0.80	-0.73	-0.76
	(-11.96)	(-11.97)	(-12.37)	(-11.94)	(-12.22)	(-11.43)	(-11.56)	(-11.88)	(-11.85)	(-11.98)	(-11.92)	-(12.39)	(-11.94)	(-12.01)	(-11.98)
4	-0.69	-0.69	-0.30	-0.71	-0.44	-1.28	-1.14	-0.83	-0.88	-0.68	-0.75	-0.33	-0.72	-0.65	-0.68
	(-12.51)	(-12.51	(-12.90	(-12.49)	(-12.76)	(-11.92)	(-12.06)	(-12.37)	(-12.32)	(-12.52)	(-12.45)	(-12.87)	(-12.48)	(-12.55)	(-12.52)
5	-0.51	-0.51	-0.06	-0.54	-0.26	-1.22	-1.08	-0.69	-0.74	-0.50	-0.59	-0.06	-0.56	-0.47	-0.50
	(-13.69)	(-13.69)	(-14.14)	(-13.66)	(-13.94)	(-12.98)	(-13.12)	(-13.51)	(-13.46)	(-13.70)	(-13.61)	-(14.14)	(-13.64)	(-13.73)	(-13.70)
6	-0.60	-0.60	-0.19	-0.63	-0.36	-1.37	-1.22	-0.85	-0.94	-0.60	-0.70	-0.28	-0.65	-0.58	-0.60
	(-13.99	(-13.99)	(-14.40)	(-13.96)	(-14.23)	(-13.22)	(-13.37)	(-13.74)	(-13.65)	(-13.99	(-13.89)	-(14.31	(-13.94)	(-14.01)	(-13.99)
7	-0.84	-0.84	-0.41	-0.87	-0.60	-1.61	-1.46	-1.08	-1.14	-0.83	-0.94	-0.45	-0.90	-0.81	-0.83
	(-14.16)	(-14.16)	(-14.59)	(-14.13)	(-14.40)	(-13.39)	(-13.54)	(-13.92)	(-13.86)	(-14.17)	(-14.06)	(-14.55)	(-14.10)	(-14.19)	(-14.17)
8	-0.66	-0.65	-0.15	-0.69	-0.42	-1.57	-1.41	-0.94	-0.99	-0.65	-0.78	-0.15	-0.72	-0.63	-0.65
	(-15.33)	(-15.34)	(-15.84)	(-15.30)	(-15.57)	(-14.42)	(-14.58)	(-15.05)	(-15.00)	(-15.34)	(-15.21)	(-15.84)	(-15.27)	(-15.36)	(-15.34)

Table 4: Differences between experimental and calculated orbital energies of butane, defined as $E_{exp} - E_{METHOD}$ of the *Group D* class (in parenthesis are the calculated energies)

HOMO-n, n=	M05	M06	M06-HF	M06-L	M08-HX	M11	M11-L	M15	M15-L	M05-2X	M06-2X	MN12-SX	MN15	N12-SX	PW6B95
	-0.01	0.09	1.22	-0.23	0.59	0.50	-0.12	0.33	-0.01	0.59	0.59	0.20	0.33	0.04	0.16
0	(-11.08)	(-11.18)	(-12.31)	(-10.86)	(-11.68)	(-11.59)	(-10.97)	(-11.42)	(-11.08)	(-11.68)	(-11.68)	(-11.29)	(-11.42)	(-11.13)	(-11.25)
	-0.53	-0.39	1.09	-0.69	0.04	-0.01	-0.43	-0.24	-0.56	0.13	0.04	-0.29	-0.24	-0.47	-0.40
2	(-11.13)	(-11.27)	(-12.75)	(-10.97)	(-11.70)	(-11.65)	(-11.23)	(-11.42)	(-11.10)	(-11.79)	(-11.70)	(-11.37)	(-11.42)	(-11.19)	(-11.26)
	-0.85	-0.66	0.56	-0.96	-0.25	-0.35	-0.60	-0.52	-0.82	-0.27	-0.25	-0.57	-0.52	-0.78	-0.71
2	(-11.45)	(-11.64)	(-12.86)	(-11.34)	(-12.05)	(-11.95)	(-11.70)	(-11.78)	(-11.48)	(-12.03)	-12.05)	(-11.73)	(-11.78)	(-11.52)	(-11.59)
	-0.85	-0.81	0.96	-1.11	-0.24	-0.24	-1.00	-0.56	-0.93	-0.14	-0.24	-0.65	-0.56	-0.80	-0.70
3	(-11.89)	(-11.93)	(-13.70)	(-11.63)	(-12.50)	(-12.50)	(-11.74)	(-12.18)	(-11.81)	(-12.60)	(-12.50)	(-12.09)	(-12.18)	(-11.94)	(-12.04)
	-0.79	-0.71	0.87	-1.02	-0.15	-0.16	-0.85	-0.49	-0.85	-0.08	-0.15	-0.56	-0.49	-0.73	-0.65
4	(-12.41)	(-12.49)	(-14.07)	(-12.18)	(-13.05)	(-13.04)	(-12.35)	(-12.71)	(-12.35)	(-13.12)	(-13.05)	(-12.64)	(-12.71)	(-12.47)	(-12.55)
	-0.62	-0.58	1.43	-0.96	0.10	0.16	-0.82	-0.26	-0.70	0.24	0.10	-0.41	-0.26	-0.55	-0.45
5	(-13.58)	(-13.62)	(-15.63)	(-13.24)	(-14.30)	(-14.36)	(-13.38)	(-13.94)	(-13.50)	(-14.44	(-14.30)	(-13.79)	(-13.94)	(-13.65)	(-13.75)
	-0.77	-0.63	1.06	-1.03	0.01	0.00	-0.71	-0.37	-0.76	0.07	0.01	-0.47	-0.37	-0.67	-0.59
6	(-13.82)	(-13.96)	(-15.65)	(-13.56)	(-14.60)	(-14.59)	(-13.88)	(-14.22)	(-13.83)	(-14.66)	(-14.60)	(-14.12)	(-14.22)	(-13.92)	(-14.00)
	-0.98	-0.91	1.00	-1.30	-0.22	-0.18	-1.08	-0.60	-1.04	-0.11	-0.22	-0.73	-0.60	-0.89	-0.81
7	(-14.02)	(-14.10)	(-16.00)	(-13.70)	(-14.78)	(-14.82)	(-13.92)	(-14.40)	(-13.96)	(-14.89)	(-14.78)	(-14.27)	(-14.40)	(-14.11)	(-14.19)
	-0.81	-0.75	1.57	-1.24	0.04	0.15	-1.08	-0.32	-0.85	0.24	0.04	-0.57	-0.32	-0.71	-0.60
8	(-15.18)	(-15.24)	(-17.56)	(-14.75)	(-16.03)	(-16.14)	(-14.91)	(-15.67)	(-15.14)	(-16.23)	(-16.03)	-15.42)	(-15.67)	(-15.28)	(-15.39)

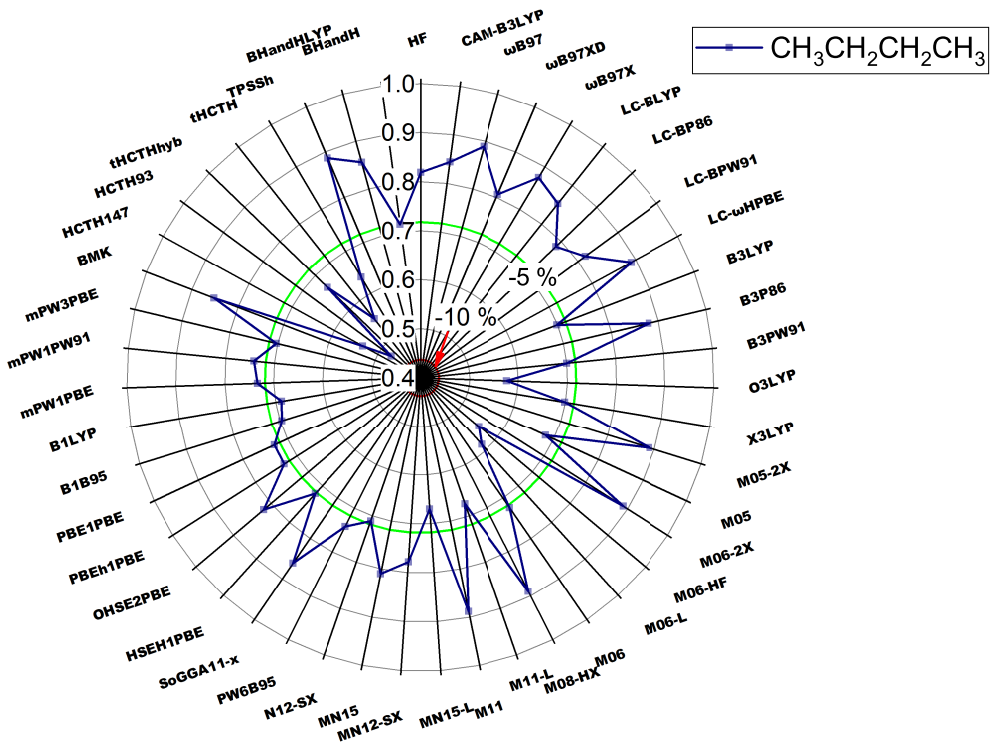

Figure 1: Similarity of calculated values with a number of theoretical approaches towards experimental findings for butane. The green (red) line denotes the similarity between experimental values and an artificial data produced as 5 % (10 %) of these values. The results that are more proximal to periphery are the most similar to experimental value.

Figure 2: Clusters of methods after obtaining the minimum spanning tree for butane.

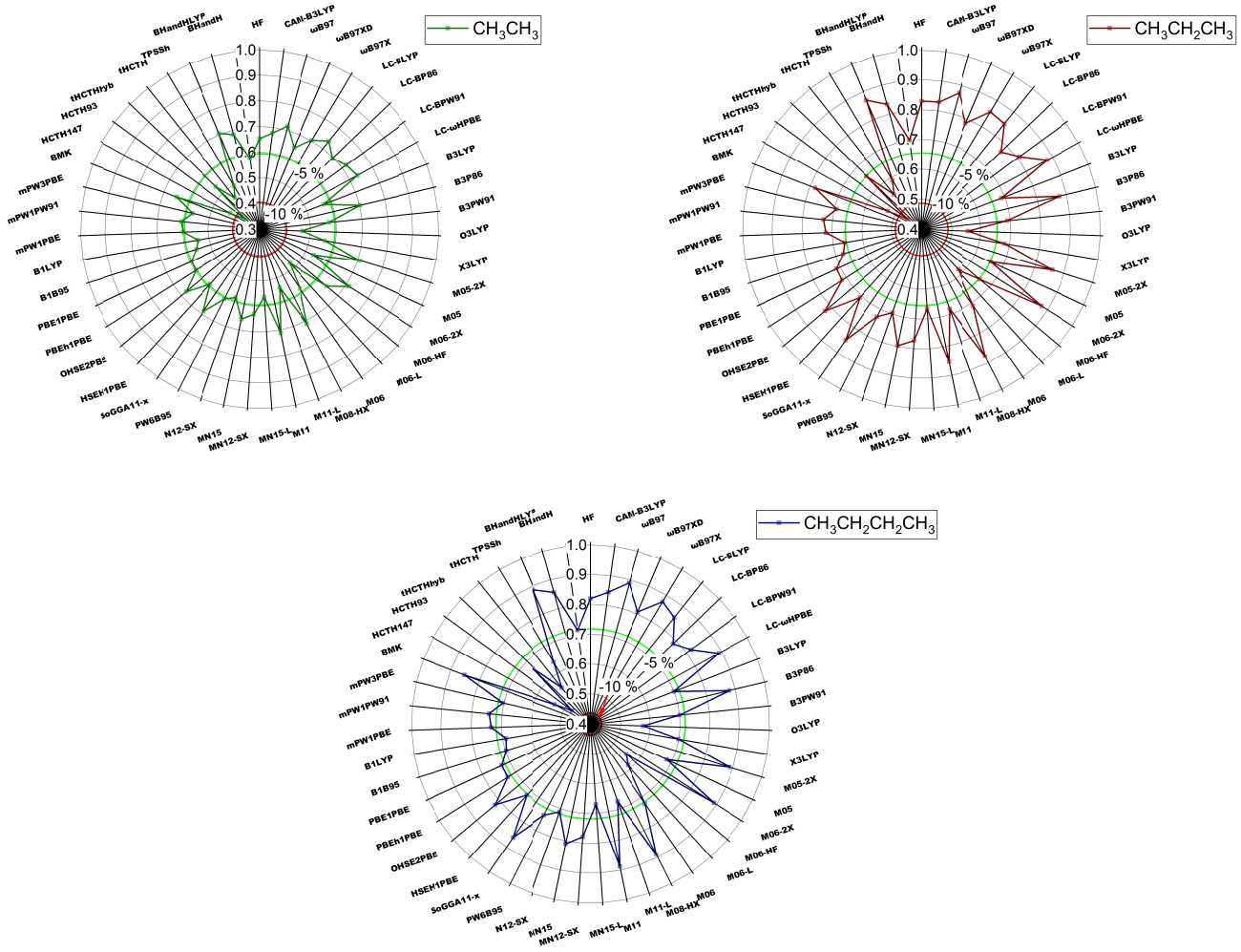

Figure 3: Similarity of calculated findings, with a number of theoretical approaches towards experimental results for ethane, propane and butane. The green (red) line denotes the similarity between experimental values and an artificial data produced as 5 % (10 %) of these values.

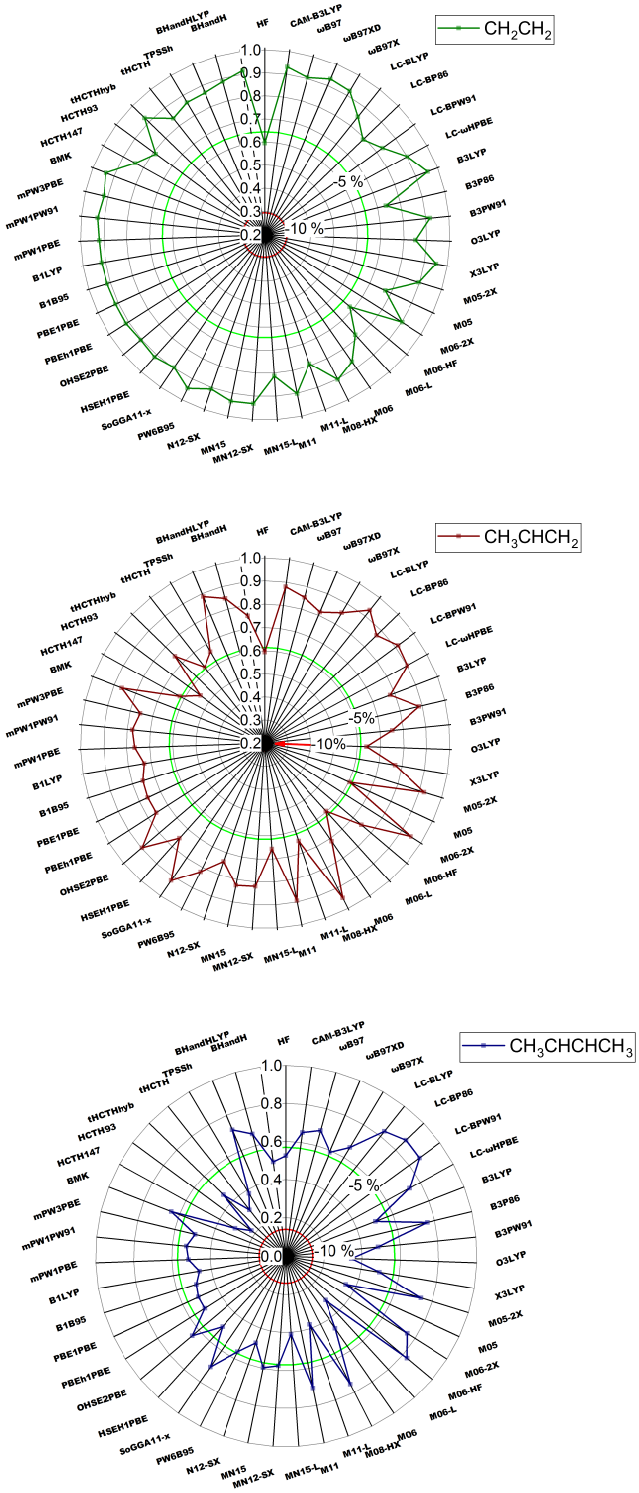

Figure 4: Similarity of calculated findings with a number of theoretical approaches towards experimental results for ethylene, propene and 2-butene. The green (red) line denotes the similarity between experimental values and an artificial data produced as 5 % (10 %) of these values.

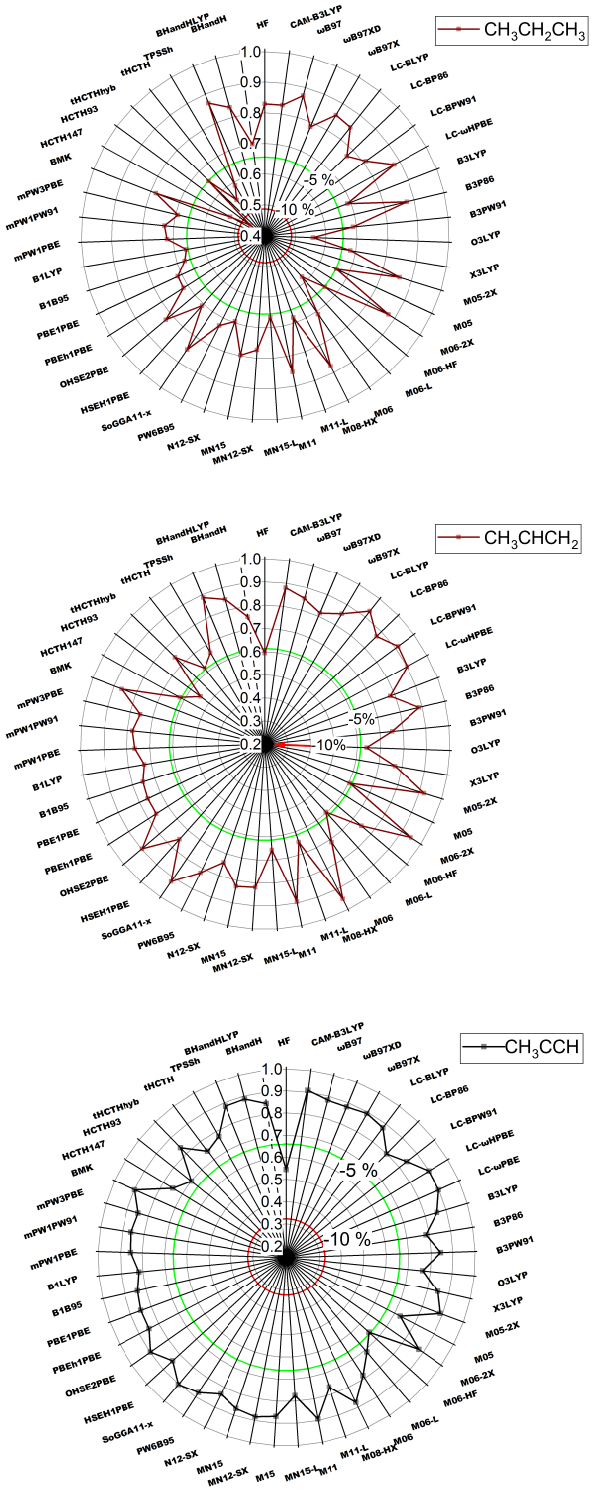

Figure 5: Similarity of calculated findings with a number of theoretical approaches towards experimental results for propane, propene and propyne. The green (red) line denotes the similarity between experimental values and an artificial data produced as 5 % (10 %) of these values.

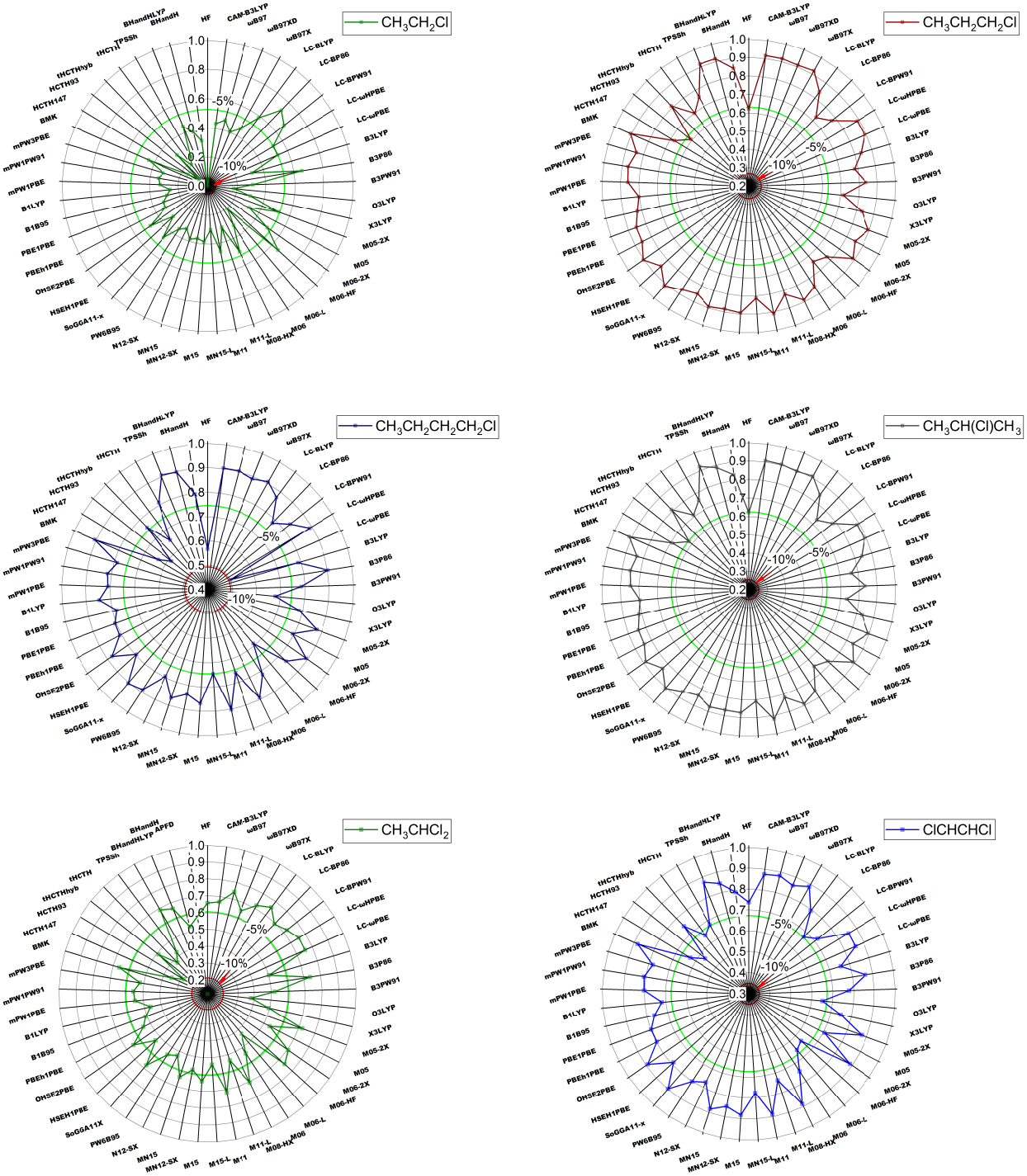

Figure 6: Similarity of calculated findings with a number of theoretical approaches towards experimental results for chloro- substituted hydrocarbons.

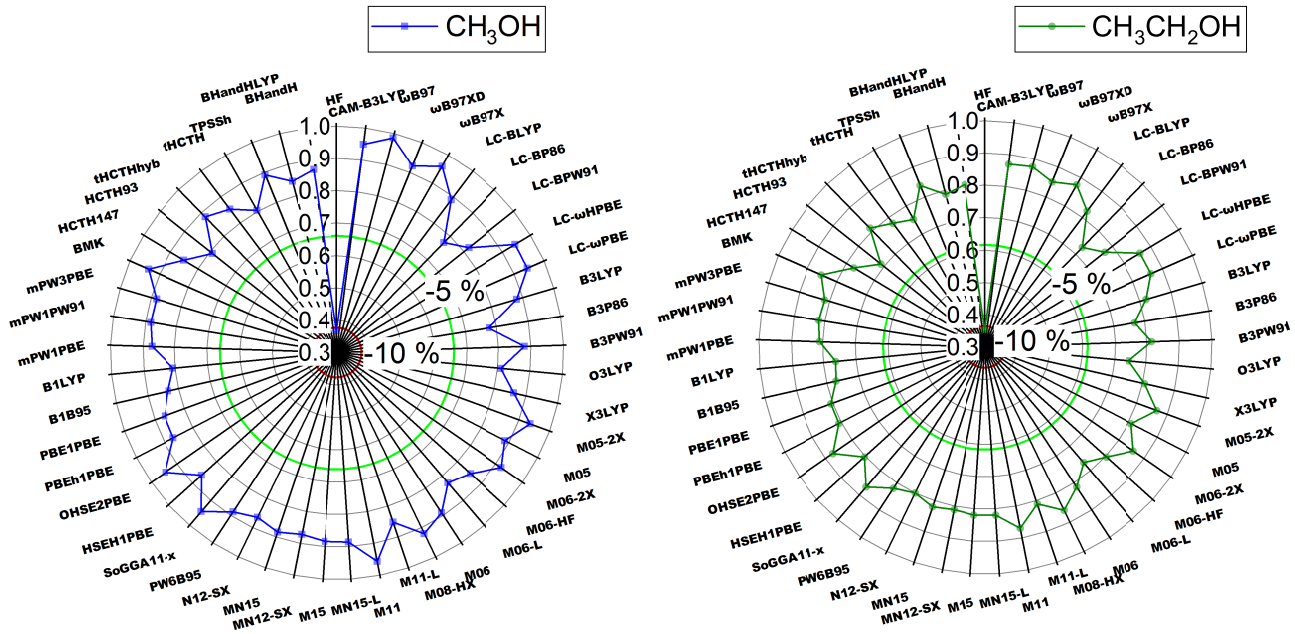

Figure 7: Similarity of calculated findings with a number of theoretical approaches towards experimental results of methanol and ethanol.